An empirical dynamic model of Hall-effect sensors

An empirical dynamic model of Hall-effect sensors

M Crescentini[1,2], and P A Traverso[1]

[1] DEI, University of Bologna, Viale del Risorgimento 2, Bologna, Italy
[2] ARCES, University of Bologna, Via Venezia 52, Cesena, Italy

m.crescentini@unibo.it

Abstract. We present an empirical, equivalent, dynamic model of Hall-effect sensors that is based on a parallel circuit composed of a controlled current generator, a resistor, and a capacitor. This solution provides optimal description of the dynamic response of the probe and easily takes into account the loading and parasitic capacitive effects. The proposed model is verified against empirical AC measurements to demonstrate the quality of the model in dynamic conditions.

1. Introduction

Hall effect-based sensors are affected by many non-idealities that degrade the measurement result but one can easily cope with them by exploiting the integration with electronic circuits [1]. However, to be effective, the compensation circuits must be adequately designed on the basis of the probe[1] behavior and requirements; therefore, the development of an accurate and reliable predictive model of the Hall-effect probe is essential. From a more general standpoint, a good model improves the knowledge about the relationships among the measurand, the main influence quantities and the output estimate, allowing to reduce the uncertainty of the measurement. The majority of the models of Hall-effect probes require many physical and technological parameters to be extracted [2,3]; thus, making them quite complex. More importantly, state-of-the-art models usually neglect the dynamic behavior of the probe [2] and only a few of them consider the parasitic capacitance due to the depletion region [3] and the loading effects of the surrounding electronics. This is in contrast with the modern trend of broadband sensing that requires good dynamic models.

In this paper, we propose an empirical, circuit-based dynamic model of Hall-effect sensors that implements the two different flows of charges that superimpose throughout the probe and describe both the static and dynamic response of the probe. The paper is organized as follow: Section II discusses the physical background, Section III presents the model, Section IV compares the model results with AC measurements made on a real prototype, and Section V draws the conclusion.

2. Physics-based considerations

In this Section, we will refer to a generic Hall-effect probe realized by a n-type well surrounded by a p-type substrate (Fig. 1-a). Two wide ohmic contacts (A and B) bias the probe and two other contacts (1 and 2) sense the Hall voltage. The substrate is connected to the global ground. The active region, that is the n-type well, is a cuboid with geometrical dimensions L, W, and t_{nom} along the x, y, and z-direction, respectively.

In static or very slowly varying operation, the standard formulation of the Hall voltage V_H is [4]

$$V_H = S_I I_{bias} B_z \qquad (1)$$

where S_I is the current-related sensitivity, I_{bias} is the bias current flowing through the probe along the x-direction, and B_z is the orthogonal component of the magnetic field. According to eq. (1), the most of the models in the literature represent the Hall voltage as a controlled voltage source [2,3], even though the main physical phenomenon behind the Hall effect is the perturbation of the charge carriers flow lines w.r.t. the trajectories for $B_z = 0$, which is due to the magnetic contribution of the Lorentz force. Indeed, the Hall voltage is basically a mere consequence of the Lorentz force $\mathbf{F_L}$ combined with the

[1] In this paper, we will use the term "probe" to refer to the semiconductor intrinsic region where the generation of the Hall voltage occurs.

boundary conditions set by the geometry and the polarization scheme of the probe. More precisely, let us assume the probe to be unbounded along the *y*-direction (i.e. $W = \infty$) and biased by a constant electric field $\mathbf{E_{bias}} = -E_{bias}\hat{\mathbf{x}}$, and let us apply a magnetic field **B** on the probe: then the total force acting on the charge carriers is given by

$$\mathbf{F_L} = -q\mathbf{E_{bias}} - q\left(\mathbf{v_n} \times \mathbf{B}\right), \qquad (2)$$

where q = 1.6x10^{-19} C is the electron charge and $\mathbf{v_n}$ is the local average velocity of the electrons. By multiplying eq. (2) by the electron mobility μ_n and the electron spatial density n, and inverting the sign, we can express the total electron current density $\mathbf{J_n}$ in implicit form as

$$\mathbf{J_n} = \mu_n nq\mathbf{E_{bias}} + \mu_n nq\left(\mathbf{v_n} \times \mathbf{B}\right) = \mathbf{J_{bias}} + \mathbf{J_{mag}} = -J_{bias}\hat{\mathbf{x}} - \mu_n\left(\mathbf{J_n} \times \mathbf{B}\right), \qquad (3)$$

where the electrostatic part is $\mathbf{J_{bias}} = -J_{bias}\hat{\mathbf{x}}$ and the magnetic part is $\mathbf{J_{mag}} = -\mu_n\left(\mathbf{J_n} \times \mathbf{B}\right)$, since $\mathbf{J_n} = -qn\mathbf{v_n}$. We can easily express the *y* component of $\mathbf{J_n}$ as $J_{ny} = \mu_n J_{nx} B_z = J_L$ by solving the vector product in (3) and assuming $J_{nz} \approx 0$. This last equation is generally true whatever the $\mathbf{B}(\mathbf{r},t)$ applying on the probe and identifies a current J_L along the *y*-direction that is due to the magnetic part of the Lorentz force but does not explicitly imply the presence of the Hall voltage (which is zero as far as the problem is *y*-unbounded).

Now, let us introduce boundary conditions: namely a finite width *W* of the probe and the presence of (floating) contacts 1 and 2, so that $J_{ny} = 0$ at the *y*-boundaries of the probe in steady state. From a general standpoint, such conditions perturb the component J_{ny} w.r.t. the unbounded regime J_L. We model this perturbative effect by introducing an equivalent current term that superimposes to J_L so that $J_{ny} = J_L - J_H$. This term is the Hall current density J_H that flows in the opposite direction from J_L and is generated by the accumulation of charges in proximity and at the *y*-boundaries of the probe. Summarizing, the magnetic part of the Lorentz force moves the electrons in the *y*-direction and accumulates them on one side of the probe, because of the boundary conditions. The accumulate charge originates the Hall electric field $\mathbf{E_H}$ and its associated equivalent current $\mathbf{J_H}$. Following this reasoning, we can write the Hall voltage as

$$V_H = -\int_W^0 \mathbf{E_H} \cdot \mathbf{dl} = \int_0^W \frac{1}{\sigma}\mathbf{J_H} \cdot \mathbf{dl} = \frac{1}{\sigma t}\frac{W}{L} I_{Hall} = R_{eq} I_{Hall}, \qquad (4)$$

where σ (assumed uniform) is the conductivity of the n-type well, *t* is the effective thickness of the well taking into account the depletion region at the p-n interface [2], and R_{eq} is the resistance seen between contacts 1 and 2. The equivalent current I_{Hall} is the current due to the accumulation of charges at the boundaries, while the unbounded regime J_L can be propagated up to terminals 1 and 2 as an equivalent current I_L (see next Section), which represents the drift of charges due to the magnetic part of the Lorentz force. These two currents are obviously equal in steady-state conditions; whereas they are unbalanced and mutually related by an ordinary differential equation in dynamic conditions, since the accumulation process is described by non-zero time constants.

3. Definition of the equivalent circuit-based dynamic model

On the basis of the above discussion, the intrinsic Hall-effect probe can be circuit-equivalently modelled as a parallel circuit (Fig. 1-b) composed of *i*) a controlled *current* generator I_L, *ii*) a capacitor *C* that describes the overall charge accumulation process, and *iii*) a resistor R_{eq} that transforms the Hall current I_{Hall} into V_H as in eq. (4). This model has full physical background, as demonstrated in Section II, is compatible with the standard formulation of the Hall voltage in steady state, and is particularly suitable for the description of the dynamic response of the probe [5]. More precisely, it explicitly shows the RC time constant that rules the dynamic operation of the probe, which has been recently demonstrated in the literature [5,6]. The dynamic response is a very important point but the most of the models in the literature either neglect it [2] or somehow embed its description within the mathematical formulation of the controlled voltage source [3]. To be more precise, the capacitance in parallel to R_{eq} is given by the sum of C_{acc} and C_j, the first being the actual capacitor describing the accumulation at the boundaries, while the latter accounts for the parasitic reversed-biased p-n junction that surrounds the active region. By integrating the unbounded regime $J_L = \mu_n J_{nx} B_z$ with the assumption of a homogeneous vertical magnetic field all over the active region, we can write the current

$$I_L = K \cdot I_{bias} \cdot B_z, \qquad (5)$$

where *K* is an empiric constant accounting for the combination of many physical parameters [4].

In order to complete the intrinsic model of the probe (Fig. 1–b), the well-known additive offset voltage V_{OS} must be taken into account. The offset is generated by asymmetries in the physical structure

of the probe as well as by environmental quantities such as the strain: the overall effect is a superimposed, magnetic-field independent, charge distribution throughout the active region with an associated electric field, an equivalent current density $\mathbf{J}_{OS}$ and a terminal current $I_{OS} = V_{OS} / R_{eq}$ that flows through the same region of $\mathbf{J_H}$.

The intrinsic equivalent circuit shown in Fig. 1-b can be extended by including the bias port, the magnetic port, and the parasitics (black-box region) so as to define a 3-port extrinsic model (Fig. 1-c) loaded by the equivalent capacitance C_{LOAD} of the embedding electronic circuits (bias and readout). It is worth noticing that the output voltage of the probe, while still preserving the superposition between Hall effect and offset, is perturbed by the parasitic network, and deviates from the intrinsic voltage on C. For the sake of simplicity, the notation $V_{OUT} = V_H + V_{OS}$ is preserved. From the bias standpoint, the Hall-effect probe behaves as a standard resistor $R_{bias} = (1/\sigma t)(L/W)$.

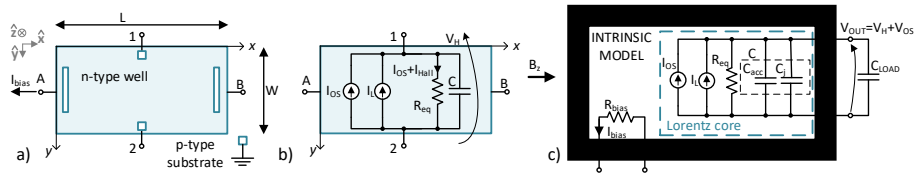

Figure 1 a) Design of a general rectangular Hall-effect probe. b) Illustration of the intrinsic "Lorentz" model superimposed to the physical probe. c) Proposed 3-port, circuit-based dynamic model of the Hall-effect probe.

4. Parameter extraction and model validation

In this Section, we will consider a squared CMOS Hall-effect probe, which is realized in 160-nm BCD (Bipolar, CMOS, DMOS) technology and employed as a current sensor. A full description of the prototype can be found in [6] (batch-a). The Hall-effect probe is realized beneath a metal strip carrying the current I to be measured (Fig. 2-a). The current I instantaneously generates the magnetic field **B** that applies to the probe. Thus, in this case study, we can replace the magnetic port in Fig. 1-c with an electric port (Fig. 2-b and Fig. 2-c). This also implies a change into eq. (5)

$$I_L = S \cdot I_{bias} I, \qquad (6)$$

where the magnetic field is replaced by the measurand I and S is the relative sensitivity.

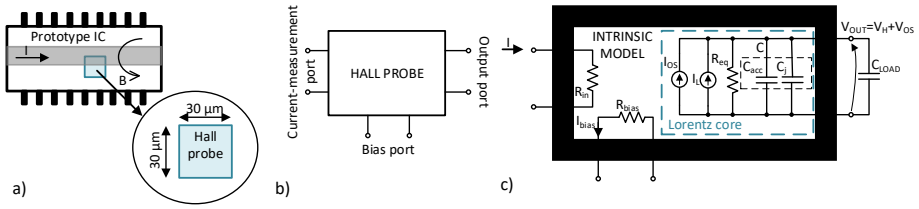

Figure 2 a) Schematic illustration of the realized prototype. b) 3-port model where the magnetic port has been replaced by the current-measurement port. c) Proposed circuit-based, equivalent electrical model.

The model parameters are extracted from either empirical measurement procedures or numerical simulations. Fig. 3 summarizes the setups for parameter extraction and highlights whether the extraction is performed by means of simulations or actual measurements. Values of the extracted parameters are summarized in the table included in Fig. 3.

The proposed model was implemented in a SPICE simulator and compared to AC measurements to demonstrate its capability of predicting the dynamic response of the Hall-effect probe. Measurements were performed by applying a reference AC current wave to the probe and recording the output voltage by an oscilloscope after amplification by means of an instrumentation amplifier with a total gain equal to 1838. The parasitic capacitance facing to the output port of the Hall-effect probe was estimated to be C_{LOAD} = (76±15) pF and takes into account the input capacitance of the instrumentation amplifier as well as all the parasitic capacitive loads due to the test-bench.

Fig. 4-a and Fig.4-b compare model predictions with measurements when the probe is excited by low-frequency signals, i.e., a 1-kHz sine wave and a 500-Hz square wave, respectively. These two tests demonstrate the quality of the model in the quasi-static regime. Fig. 4-c and Fig. 4-d compare model predictions with measurements when the Hall-effect probe is excited with high-frequency signals, i.e., a 120-kHz current sine wave and a positive edge of a periodic pulse. In these cases, the dynamic regime is fully excited and the dynamic parasitic elements are no longer negligible: to improve the accuracy of

model predictions, spurious emfs [5] and capacitive coupling between the measurement port and output port must be characterized and dealt with in the black-box of Figs. 1-c and 2-c. These parasitic elements are tightly related to the practical realization of the prototype. Moreover, the predicted response in Fig. 4-d was obtained by recording the samples of the stimulus current signal and using them as input to SPICE model. This procedure allows to compare model prediction with measurement result in an easier way but also adds noise to the simulation result. The proposed model demonstrates to accurately predict the amplitude response to the sine wave excitation, but with a small deviation in the phase response (Fig. 4-c); while the inclusion of the parasitic elements (black box) allows for a very good prediction of glitches shown in Fig. 4-d.

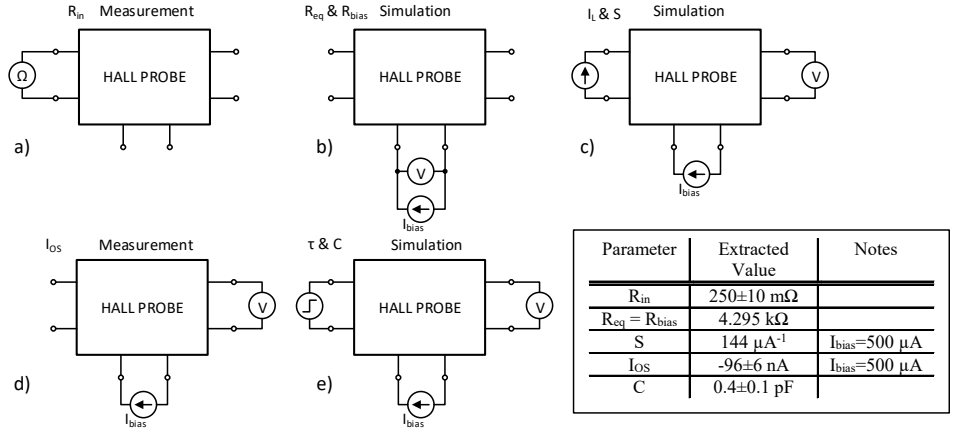

Parameter	Extracted Value	Notes
R_{in}	250±10 mΩ	
$R_{eq} = R_{bias}$	4.295 kΩ	
S	144 μA^{-1}	I_{bias}=500 μA
I_{OS}	-96±6 nA	I_{bias}=500 μA
C	0.4±0.1 pF	

Figure 3 Schematics of the setups for the extraction of model parameters: a) R_{in}, b) R_{eq} and R_{bias}, c) S, d) I_{OS}, and e) C. The extracted values are summarized in the table.

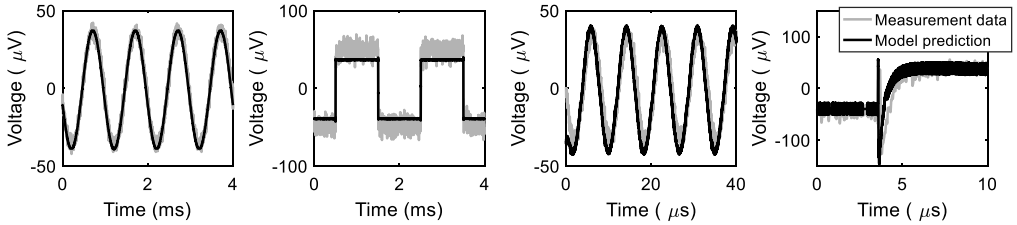

Figure 4 Comparison of model simulations Vs. AC measurement data on the prototype when excited with a) 1-kHz sine wave, b) 500-Hz square wave, c) 120-kHz sine wave, and d) positive edge of a periodic pulse train.

5. Conclusion

An empirical, circuit equivalent-based dynamic model of Hall-effect probe was proposed, which explicitly describes the flows of charge carriers throughout the probe due to the Lorentz force and the Hall effect. With respect to the state of the art, the proposed model is suitable to predict also the dynamic operation of the probe and allows to take into account the loading effect of the readout circuit. Future work will be devoted to the improvement of the model by implementing the static non-linearity due to the thickness-bias relation and other second-order effects like the magnetoresistivity.

Acknowledgments

This work was founded from the ECSEL Joint Undertaking (JU) under grant agreement No 737434.

References

[1] Crescentini M, Marchesi M, Romani A, Tartagni M and Traverso P A 2018 A Broadband, On-Chip Sensor Based on Hall Effect for Current Measurements in Smart Power Circuits *IEEE Trans. Instrum. Meas.* **67** 1470–85
[2] Madec M, Kammerer J B, Hébrard L and Lallement C 2011 An accurate compact model for CMOS cross-shaped Hall effect sensors *Sensors Actuators A. Phys.* **171** 69–78
[3] Xu Y and Pan H-B 2011 An improved equivalent simulation model for CMOS integrated Hall plates. *Sensors.* **11** 6284
[4] Crescentini M, Biondi M, Romani A, Tartagni M and Sangiorgi E 2017 Optimum Design Rules for CMOS Hall Sensors *Sensors* **17** 765
[5] Crescentini M, Marchesi M, Romani A, Tartagni M and Traverso P A 2017 Bandwidth Limits in Hall Effect-based Current Sensors *Acta-IMEKO* **6** 17–24
[6] Crescentini M, Traverso P A, Alberti P, Romani A, Marchesi M, Cristaudo D, Canegallo R and Tartagni M 2016 Experimental characterization of bandwidth limits in hall sensors *21st IMEKO TC-4 Int. Symposium* (Budapest, Hungary) pp 1–6